Unc5B associates with LARG to mediate the action of repulsive guidance molecule

Katsuhiko Hata,[1] Kozo Kaibuchi,[3] Shinobu Inagaki,[2] and Toshihide Yamashita[1]

[1]Department of Molecular Neuroscience and [2]Group of Neurobiology, Division of Health Sciences, Osaka University Graduate School of Medicine, Suita, Osaka 565-0871, Japan
[3]Department of Cell Pharmacology, Graduate School of Medicine, Nagoya University, Nagoya, Aichi 466-8550, Japan

Neuronal axons are guided by attractive and repulsive cues in their local environment. Because the repulsive guidance molecule A (RGMa) was originally identified as an axon repellent in the visual system, diverse functions in the developing and adult central nervous system have been ascribed to it. RGMa binding to its receptor neogenin induces RhoA activation, leading to inhibitory/repulsive behavior and collapse of the neuronal growth cone. However, the precise mechanisms that regulate RhoA activation are poorly understood. In this study, we show that Unc5B, a member of the netrin receptor family, interacts with neogenin as a coreceptor for RGMa. Moreover, leukemia-associated guanine nucleotide exchange factor (LARG) associates with Unc5B to transduce the RhoA signal. Focal adhesion kinase (FAK) is involved in RGMa-induced tyrosine phosphorylation of LARG as well as RhoA activation. These findings uncover the molecular basis for diverse functions mediated by RGMa.

Introduction

In the nervous system, axons are guided by attractive and repulsive cues in the extracellular matrix. When these cues are detected by specific receptors present on growth cones and neurites, intracellular signaling cascades are initiated, leading to changes in the growth cone morphology as well as the trajectory of growing fibers. The repulsive guidance molecule (RGM) was originally identified in the chick retinotectal system as a glycosylphosphatidylinositol-anchored, membrane-bound protein with repulsive properties (Monnier et al., 2002). In vertebrates, three homologues of RGM, namely, RGMa, RGMb (DRG11-responsive axonal guidance and outgrowth of neurite), and RGMc (hemojuvelin) have been identified (Niederkofler et al., 2004; Schmidtmer and Engelkamp, 2004). RGMa, which is highly homologous (80% identity) to chick RGM, functions as a repulsive guidance cue in the developing and adult central nervous system (CNS; Brinks et al., 2004; Matsunaga et al., 2004, 2006; Hata et al., 2006; Wilson and Key, 2006; Metzger et al., 2007; Tassew et al., 2008).

Neogenin, the receptor for RGMa, is a single membrane-spanning protein, a member of the Ig superfamily, and closely related to the netrin-1 receptor, deleted in colorectal cancer (DCC; Rajagopalan et al., 2004). Neogenin is broadly expressed in the embryonic and adult CNS (Gad et al., 1997; Manitt et al., 2004). The molecular mechanisms of RGMa–neogenin signaling have been identified. RGMa inhibits the neurite outgrowth of cerebellar granule neurons in a RhoA/Rho kinase-dependent manner (Hata et al., 2006). RGMa binding to neogenin activates RhoA, Rho kinase, and PKC, inducing growth cone collapse (Conrad et al., 2007). However, the mechanism of the neogenin-mediated regulation of RhoA activity remains unknown. In this study, we show that Unc5B associates with leukemia-associated guanine nucleotide exchange factor (GEF [LARG]) to mediate the signal transduction leading to growth cone collapse and RhoA activation.

Unc5B is a member of the netrin receptor Unc5 family, which includes Unc5A–D, which is also called Unc5h1–4. All members of the Unc5 family are single-pass transmembrane

Correspondence to Katsuhiko Hata: hata0731@molneu.med.osaka-u.ac.jp; or Toshihide Yamashita: yamashita@molneu.med.osaka-u.ac.jp

Abbreviations used in this paper: ANOVA, analysis of variance; CNS, central nervous system; DB, DCC binding; DCC, deleted in colorectal cancer; DD, death domain; ECD, extracellular domain; FRNK, FAK-related nonkinase; GEF, guanine nucleotide exchange factor; GPCR, G protein–coupled receptor; HEK, human embryonic kidney; ICD, intracellular domain; IGF-1, insulin-like growth factor-1; IP, immunoprecipitation; LARG, leukemia-associated GEF; RGM, repulsive guidance molecule; RGS, regulator of G protein signaling; TrkB, tropomyosin-related kinase B; VSV-G, vesicular stomatitis virus G protein.

The Rockefeller University Press $30.00
J. Cell Biol. Vol. 184 No. 5 737–750
www.jcb.org/cgi/doi/10.1083/jcb.200807029

proteins. They have a highly conserved common structure. Two Ig and thrombospondin domains are located in the extracellular region. The zona occludens (ZO)-1 and Unc5-like netrin receptor (ZU5) domain, DCC-binding (DB) domain, and death domain (DD) are located in the intracellular region (Engelkamp, 2002). Unc5 is widely expressed in various embryonic and adult tissues in mammals (Engelkamp, 2002; Manitt et al., 2004). The DCC–Unc5 receptor complex initiated by netrin-1 induces long-range repulsion from netrin-1, whereas the Unc5 receptor alone transduces short-distance repulsion (Barallobre et al., 2005).

LARG is a member of the regulator of G protein signaling (RGS)–RhoGEF subfamily. A total of three RhoGEFs, namely p115RhoGEF, PDZ (PSD-95/Dlg/ZO-1 homology)-RhoGEF/GTRAP48, and LARG, have been isolated in this subfamily (Fukuhara et al., 1999, 2000). All members of this subfamily contain both Dbl/pleckstrin homology and RGS domains, but only LARG and PDZ-RhoGEF contain the PDZ domain. Although p115-RhoGEF expression is largely restricted to hematopoietic cells, LARG and PDZ-RhoGEF are widely expressed in various organs and organ systems, including the CNS (Fukuhara et al., 1999; Kourlas et al., 2000). LARG and PDZ-RhoGEF bind to the activated α subunit of the heterotrimeric guanine nucleotide-binding proteins (G proteins) $G\alpha_{12}$ and $G\alpha_{13}$ through the RGS domain, leading to the activation of RhoA (Fukuhara et al., 1999, 2001). The involvement of these RhoGEFs in RhoA activation mediated by the insulin-like growth factor-1 (IGF-1) receptor or semaphorin 4D/plexin-B1 receptor has also been reported (Taya et al., 2001; Aurandt et al., 2002; Driessens et al., 2002; Swiercz et al., 2002).

In this study, we show that Unc5B constitutively associates with neogenin as a coreceptor for RGMa. RhoA activation and growth cone collapse by RGMa were inhibited by dominant-negative Unc5B or siRNA against Unc5B. Next, Unc5B interacted with LARG to transduce the RGMa signal. Furthermore, we found that FAK was involved in RGMa-induced tyrosine phosphorylation of LARG as well as RhoA activation. Thus, Unc5B associates with neogenin to form a coreceptor for RGMa and interacts with LARG to mediate RhoA activation and growth cone collapse.

Results

Neogenin associates with Unc5B

We first examined whether neogenin interacted with Unc5B. Human embryonic kidney (HEK) 293T cells were transfected with mock, vesicular stomatitis virus G protein (VSV-G)–tagged neogenin (neogenin–VSV-G) and mock, HA-tagged Unc5B (Unc5B-HA) and mock, or neogenin–VSV-G and Unc5B-HA constructs. The cell extracts were immunoprecipitated with an anti–VSV-G or anti-HA antibody (Fig. 1, A and B). Of all the neogenin–VSV-G immunoprecipitates, the anti-HA antibody revealed the presence of Unc5B-HA only in the precipitates from neogenin–Unc5B-cotransfected cells (Fig. 1 A). Similar results were observed in the experiment in which the anti-HA antibody was used for the immunoprecipitation (IP) of Unc5B-HA (Fig. 1 B). We also observed that neogenin–VSV-G interacted with myc-tagged Unc5A (Unc5A-myc) as and Unc5C by performing co-IP with transfected 293T cells (Fig. 1, C–F). These results demonstrate that ectopically expressed neogenin interacted with Unc5 receptors in 293T cells.

We next investigated the molecular determinants of the interaction of neogenin with Unc5B. To examine the in vitro binding between the neogenin and Unc5B extracellular domains (ECDs), ELISA was performed. We added 2 μg/ml Fc-tagged recombinant Unc5B ECD (Unc5B-ECD-Fc) or BSA to plastic wells coated with 0.5 μg/ml His-tagged recombinant neogenin-ECD (neogenin-ECD-His) or BSA, respectively (Fig. 1 G, left). The mean OD value when Unc5B-ECD-Fc was added to the well coated with neogenin-ECD-His was significantly higher than those of the controls, indicating that recombinant neogenin-ECD binds directly to recombinant Unc5B-ECD in vitro. We also investigated the interaction of RGMa with Unc5B-ECD-Fc by ELISA. As reported previously, specific RGMa-Unc5B binding was not detected (Rajagopalan et al., 2004; Kuns-Hashimoto et al., 2008). To determine whether the association between ECD of neogenin and Unc5B occurred in cis or trans, we conducted cell mixing experiments using neogenin–VSV-G– and Unc5B-HA–transfected 293T cells (Fig. 1, H and I). Cell lysates were prepared from the culture of 293T cells transfected with mock, neogenin–VSV-G, or Unc5B-HA constructs and from a mixed culture of neogenin–VSV-G– and Unc5B-HA–overexpressing cells. These lysates were subjected to co-IP analysis. We did not observe co-IP of neogenin with Unc5B in the mixed cell culture. Moreover, the specific interaction of neogenin–VSV-G with Unc5B-ECD was detected in transfected 293T cells (Fig. 1, J and K). These findings suggest that neogenin-ECD interacts with Unc5B-ECD in cis.

To investigate the in vitro binding between the neogenin and Unc5B intracellular domains (ICDs), a GST pull-down assay was performed. Extracts from 293T cells that expressed various HA-tagged deletion constructs of the Unc5B ICD shown in Fig. 1 L were incubated with GST or GST-neogenin-ICD. Mutants containing the DB domain (Unc5B ICD-HA and Unc5B ZU5/DB-HA) bound to GST-neogenin-ICD, whereas those without the DB domain (Unc5B ICD-ZU5-HA and Unc5B DD-HA) did not (Fig. 1 M). These data suggested that Unc5B interacted with neogenin via its ECD and intracellular DB domain.

To characterize the interaction of endogenous neogenin and Unc5B in vivo, we examined the interaction by using lysates prepared from rat cortical neurons obtained on embryonic days (E) 19–20. IP was performed with anti-Unc5B or control antibody followed by immunoblotting with antineogenin antibody. Neogenin was detected in the immunoprecipitates obtained using anti-Unc5B antibody but not in those obtained using control IgG (Fig. 1 N). We also examined whether this interaction was regulated by RGMa bound to neogenin. The amount of neogenin detected in the immunocomplex with Unc5B did not change when the cells were stimulated with 2 μg/ml RGMa for 15 min. We confirmed that the Unc5B antibody used in this assay did not detect the overexpressed neogenin in 293T cells, supporting the specific binding of neogenin to Unc5B in cortical neurons (Fig. 1 O). Thus, neogenin constitutively interacted with Unc5B in the cortical neurons.

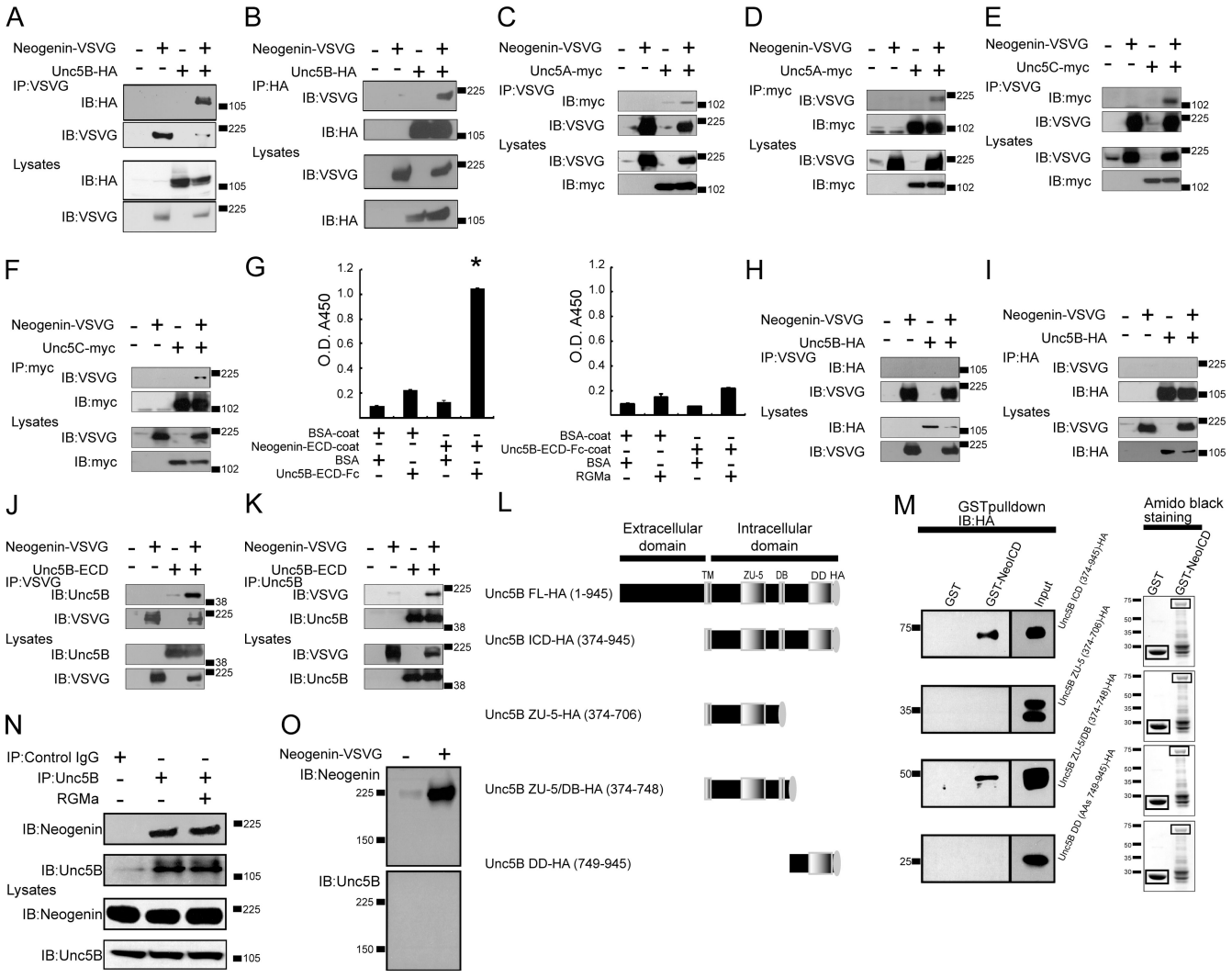

Figure 1. **Neogenin and Unc5B form receptor complexes.** (A and B) Co-IP of neogenin with Unc5B using lysates prepared from the transfected 293T cells. The immunocomplexes and cell lysates were subjected to immunoblot analysis with anti–VSV-G or anti-HA antibody. (C and D) Co-IP of neogenin with Unc5A in transfected 293T cells. The neogenin–VSV-G, Unc5A-myc, or vector alone (mock) were transfected into 293T cells. The immunocomplexes and cell lysates were subjected to immunoblot analysis with anti–VSV-G or anti-myc antibody. (E and F) Co-IP of neogenin with Unc5C in transfected 293T cells. (G, left) Binding of Unc5B-ECD-Fc to ELISA microwells coated with neogenin-ECD. Neogenin-ECD or BSA-bound Unc5B-ECD was detected by anti-Unc5B antibody. Data are represented as the mean ± SEM of three independent experiments. *, $P < 0.01$ compared with all of the other data. (right) Binding of RGMa to ELISA plates coated with Unc5B-ECD-Fc was examined. (H and I) Cell mixing experiments using neogenin–VSV-G- and Unc5B-HA–transfected cells. Cell lysates were incubated with anti–VSV-G (H) or with the anti-HA antibody (I). The immunocomplexes and cell lysates were subjected to immunoblot analysis with anti–VSV-G or anti-HA antibody. (J and K) Co-IP of neogenin with Unc5B-ECD in transfected 293T cells. Anti–VSV-G or antibody recognizing ECD of Unc5B (anti-Unc5B antibody) was used for IP and immunoblotting. (L) Schematic representation of Unc5B intracellular deletion constructs. (M) GST pull-down assay using GST-neogenin-ICD (GST-Neo-ICD) and various deletion mutants (L) of the Unc5B ICD. The proteins bound to the beads were detected with anti-HA antibody. The amido black staining of the membranes with the boxes indicates the position of the GST fusion proteins used in the pull-down assay. (N) Co-IP of Unc5B with neogenin in rat cortical neurons. Lysates were immunoprecipitated with anti-Unc5B antibody (IP:Unc5B) or control IgG (IP:Control IgG). (O) The lysates from control or neogenin-overexpressing 293T cells were subjected to immunoblot analysis probed with anti-Unc5B antibody used in N. IB, immunoblotting.

Unc5B mediates RGMa-induced RhoA activation

The interaction of neogenin and Unc5B prompted us to examine whether the latter was required for RGMa–neogenin-mediated signaling. Because it has been reported that RGMa activates RhoA in primary neurons and that this activation is dependent on neogenin (Hata et al., 2006; Conrad et al., 2007), we explored the role of Unc5B in RhoA activation by RGMa. The activity of RhoA was determined by the affinity precipitation of GTP-RhoA, using the RhoA-binding domain of the effector protein rhotekin (Ren and Schwartz, 2000).

We first used 293T cells, which endogenously express the RhoGEF responsible for RGMa-induced RhoA activation (LARG; see the following section) but express considerably lower levels of neogenin and Unc5B (Fig. 2 C and see Fig. 5 A; Wang et al., 2004b; Lee et al., 2007). The cells were transiently transfected with mock, neogenin and mock, Unc5B and mock, neogenin and Unc5B, or neogenin and Unc5B-ECD constructs (Fig. 2 A). The RhoA activation assay was performed in the presence and absence of 2 µg/ml RGMa. Cells expressing the mock construct either alone or in combination with neogenin–VSV-G or Unc5B-HA did not show a significant change in the

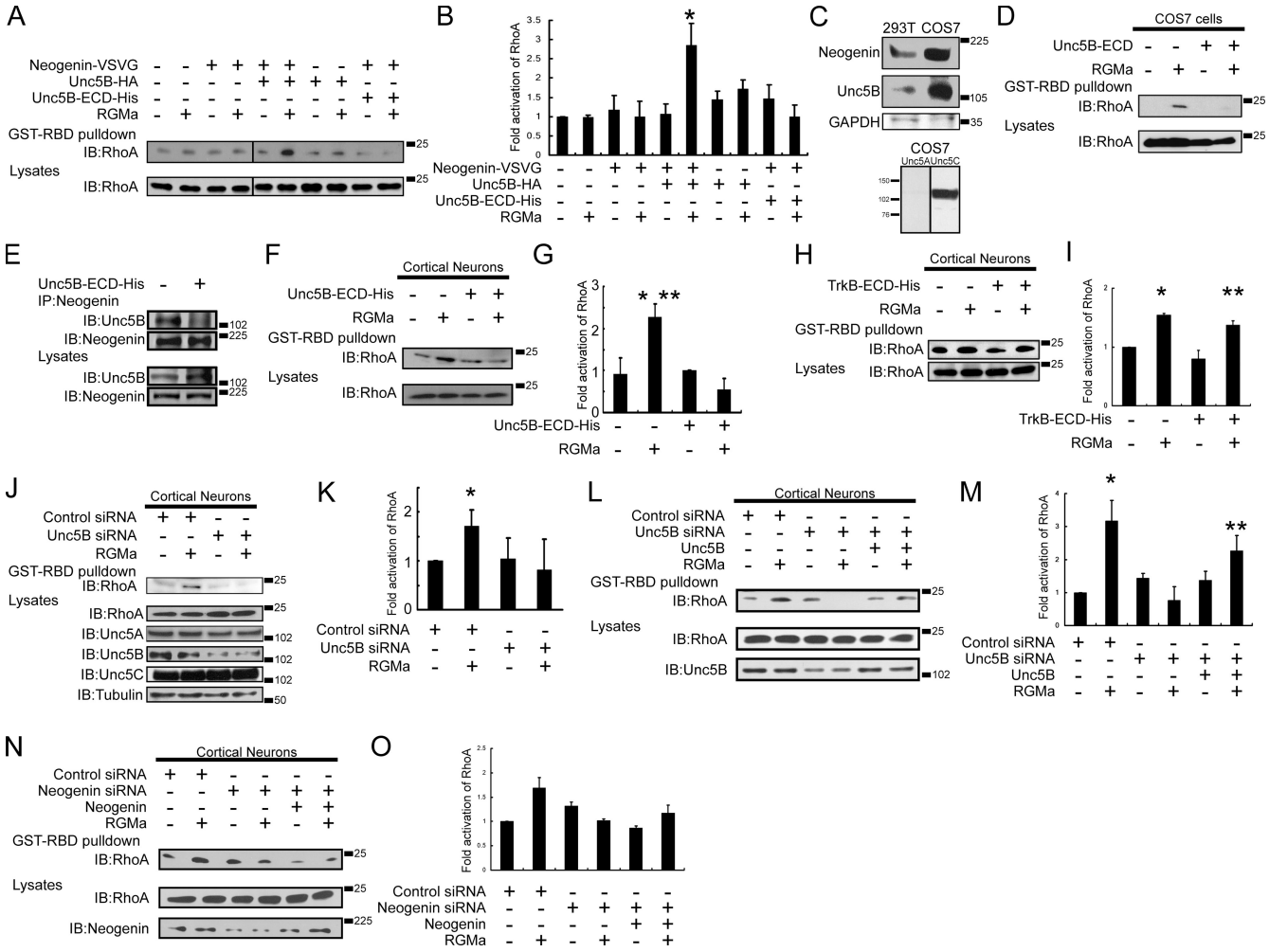

Figure 2. **Involvement of Unc5B in RhoA activation by RGMa.** (A) Affinity precipitation of GTP-RhoA in the 293T cells transfected with mock, neogenin and mock, Unc5B and mock, neogenin and Unc5B, or neogenin and Unc5B-ECD constructs. (top) Transfected cells were treated with or without 2 µg/ml RGMa for 15 min, lysed, and subjected to rhotekin pull-down assays to detect the active form of RhoA. (bottom) Whole cell lysates were also immunoblotted with anti-RhoA antibody. RhoA activity is indicated by the amount of rhotekin-bound RhoA normalized to the amount of RhoA in the lysates. (B) The quantification of the data in A from three independent experiments. *, $P < 0.05$ compared with neogenin(+)/Unc5B(+)/Unc5B-ECD-His(−)/RGMa(−) or (+)/(−)/(+)/(+). RGMa elicits the activation of RhoA only when 293T cells express neogenin and Unc5B. (C, top) Immunoblotting of 293T cells and COS-7 cells for neogenin, Unc5B, and glyceraldehyde 3-phosphate dehydrogenase (GAPDH). (bottom) Immunoblotting of COS-7 cells for Unc5A and Unc5C. (D) RhoA activation assay in the COS-7 cells transfected with mock or Unc5B-ECD constructs. (E) Co-IP of neogenin with Unc5B from rat cortical neurons treated with purified Unc5B-ECD-His or control medium for 48 h. (F and G) Effects of Unc5B-ECD-His on RhoA activation by RGMa in cortical neurons. (G) The quantification of the data in F from three independent experiments *, $P < 0.05$ compared with Unc5B-ECD-His(−)/RGMa(−); **, $P < 0.01$ compared with (+)/(+). (H) Effects of TrkB-ECD-His on RhoA activation by RGMa in cortical neurons. (I) The quantification of the data in H from three independent experiments. *, $P < 0.01$ compared with TrkB-ECD-His(−)/RGMa(−); **, $P < 0.01$ compared with (+)/(−). (J) Effects of knockdown of Unc5B expression on RhoA activation by RGMa in cortical neurons. Western blots of the lysates panel show specific knockdown of Unc5B expression by its siRNA. The expression of Unc5A or Unc5C was not reduced. (K) The quantification of the data in J from three independent experiments. *, $P < 0.05$ compared with control siRNA(−)/Unc5B siRNA(+)/RGMa(+). (L) Unc5B siRNA rescue experiment. Neurons were cotransfected with control siRNA and mock construct, Unc5B siRNA and mock construct, or Unc5B siRNA and Unc5B-HA construct. Western blots of the lysates panel show that knockdown of Unc5B expression by Unc5B siRNA was rescued by transfection of a plasmid encoding Unc5B-HA but not by mock plasmid. (M) The quantification of the data in L from three independent experiments. *, $P < 0.05$ compared with control siRNA(+)/Unc5B siRNA(−)/Unc5B(−)/RGMa(−) or (−)/(+)/(−)/(+); **, $P < 0.05$ compared with (−)/(+)/(+)/(−). (N) Effects of knockdown of neogenin expression on RhoA activation by RGMa in cortical neurons. (O) The quantification of the data in N from three independent experiments. Error bars indicate SEM. IB, immunoblotting.

RhoA activity in response to RGMa. In contrast, cotransfection with neogenin–VSV-G and Unc5B-HA resulted in a significant increase in the RGMa-induced RhoA activity (Fig. 2, A and B). In addition, cotransfection with neogenin–VSV-G and Unc5B-ECD constructs did not lead to an increase in the RGMa-induced RhoA activity. These data showed that Unc5B, especially its ICD, was required for RGMa-induced RhoA activation in 293T cells.

We next investigated the role of Unc5B in RGMa-induced RhoA activation by using COS-7 cells and rat primary cortical neurons, both of which endogenously express neogenin and Unc5 receptors (Fig. 1 N; and Fig. 2, C and J) and LARG (the expression of LARG in COS-7 cells; see Fig. 5 E and not depicted). As our data demonstrate that Unc5B-ECD directly interacts with neogenin (Fig. 1 G) and that the interaction of endogenous neogenin with Unc5B in cortical neurons is inhibited by the

addition of Unc5B-ECD-His (Fig. 2 E), Unc5B-ECD-His may function as a dominant-negative inhibitor of endogenously expressed Unc5B and block the RGMa signaling pathway. To test this possibility, rat cortical neurons (E19–20) were cultured for 48 h with Unc5B-ECD-His, recombinant tropomyosin-related kinase B (TrkB)–His, or control solution and treated with 2 µg/ml RGMa or control medium; the activity of RhoA was then measured. As shown in Fig. 2 (F–I), the RhoA activation induced by RGMa was blocked by the introduction of Unc5B-ECD-His but by control medium or TrkB-His. Similar results were obtained on performing the Rho assay in COS-7 cells transfected with the mock construct or Unc5B-ECD-HA (Fig. 2 D). Furthermore, we found that the RGMa-elicited RhoA activation in cortical neurons was inhibited by the transfection of siRNA against Unc5B (Lee et al., 2007). This activation was not inhibited by control nontargeting siRNA (Fig. 2, J and K). Identical results were obtained with different siRNAs targeting Unc5B (unpublished data). To test the specificity of Unc5B siRNA as well as the possible existence of off-target effects of the siRNAs on RGMa-induced RhoA activation, we performed a rescue experiment in the knocked-down neurons (Fig. 2, L and M). A total of 72 h after transfection with Unc5B-HA or mock construct into Unc5B knocked-down neurons, cells were treated with 2 µg/ml RGMa or control medium for 15 min and subjected to the RhoA activation assay. The transfection of Unc5B rescued RGMa-induced RhoA activation in Unc5B siRNA–transfected neurons, whereas the transfection of the mock construct did not. Thus, our data support the notion that the effect of Unc5B siRNA on the RGMa-elicited RhoA activation was not an off-target effect. These results suggest that Unc5B, which interacts with neogenin, transduces the signal from RGMa to RhoA.

To confirm the previous study demonstrating the involvement of neogenin in RGMa-induced RhoA activation (Conrad et al., 2007), we examined the effects of knockdown of neogenin expression on the activation of RhoA by RGMa in cortical neurons. The result showed that knockdown of neogenin by its siRNA also resulted in the elimination of RGMa-dependent RhoA activation (Fig. 2, N and O). The specificity of the effect of neogenin siRNA was also confirmed in the rescue experiment, in which neogenin knocked-down neurons were transfected with neogenin–VSV-G or mock constructs.

Unc5B is required for RGMa-induced growth cone collapse

As reported previously, RGMa induces growth cone collapse in a RhoA/Rho kinase-dependent manner (Monnier et al., 2002; Conrad et al., 2007; Kubo et al., 2008). We used this fact to estimate the involvement of Unc5B in RGMa-induced growth cone collapse by using Unc5B-ECD-His or Unc5B siRNA.

The rat cortical neurons (E19–20) were cultured for 48 h in the presence or absence of 2 µg/ml Unc5B-ECD-His. After stimulation with 2 µg/ml RGMa or control medium for 30 min, the neurons were fixed and double labeled with anti-Tuj1 and phalloidin (Fig. 3 A). The growth cones collapsed after the addition of RGMa (Fig. 3, A and B). However, in the Unc5B-ECD-His–treated neurons, the collapse induced by RGMa was significantly inhibited. Next, we examined whether the RGMa-elicited growth cone collapse was also blocked by Unc5B siRNA. Cortical neurons were transfected with Unc5B siRNA or control siRNA; 72 h later, the growth cone collapse assay was performed. Fig. 3 (C and D) shows that the knockdown of Unc5B specifically and significantly reduced the growth cone collapse in response to RGMa. Again, we performed a rescue experiment in the knocked-down neurons (Fig. 3, E and F). The rat cortical neurons were transfected with a GFP-encoding vector together with control siRNA, Unc5B siRNA, or Unc5B siRNA and Unc5B-HA constructs. The cotransfection assay revealed that the ratio of the number of GFP/plasmid to both siRNAs and rescue construct was 1:10. As described previously (Menard et al., 2002; Kubo et al., 2008), almost all GFP-positive neurons were cotransfected with both siRNAs and rescue construct. The ectopic expression of Unc5B, as checked by the GFP expression, rescued RGMa-induced growth cone collapse in Unc5B siRNA–transfected neurons, whereas the transfection of the mock construct did not.

Furthermore, we investigated the involvement of neogenin in RGMa-induced growth cone collapse. As shown in Fig. 3 (G and H), the knockdown of neogenin by transfection with neogenin siRNA, GFP, and mock constructs resulted in the specific elimination of RGMa-induced growth cone collapse. The specific effect of the neogenin siRNA was confirmed in the rescue experiment. These results indicated that Unc5B was necessary for the growth cone collapse elicited by RGMa. Thus, Unc5B associated with neogenin to form a receptor complex for RGMa.

Unc5B interacts with LARG

We next explored the missing link between the receptor complex for RGMa and RhoA activation. Rho GTPases are activated by proteins that augment GTP binding such as GEFs. Promising candidate RhoGEFs that participate in the RGMa–neogenin–Unc5B pathway are the PDZ domain–containing RhoGEFs, namely PDZ-RhoGEF and LARG. It was reported that both neogenin and DCC bind to FAK through their highly homologous ICDs (Liu et al., 2004; Ren et al., 2004) and that FAK phosphorylates PDZ-RhoGEF and LARG (Chikumi et al., 2002a). These RhoGEFs have been reported to be involved in the RhoA activation induced by the IGF-1/IGF-1 or semaphorin 4D/plexin-B1 receptors (Taya et al., 2001; Aurandt et al., 2002; Driessens et al., 2002; Swiercz et al., 2002). In addition, a member of the Unc5 receptor family, Unc5A, contains a PDZ-binding region in its C-terminal DD (Williams et al., 2003). These observations hinted at a connection between PDZ-RhoGEF or LARG and RGMa-induced RhoA activation.

We first investigated whether PDZ-RhoGEF or LARG interacted with neogenin or Unc5B by performing co-IP with transfected 293T cells. We did not observe the co-IP of neogenin with PDZ-RhoGEF, neogenin with LARG, and Unc5B with PDZ-RhoGEF (not depicted), whereas the co-IP of Unc5B with LARG was detected (Fig. 4, A and B). In the Unc5B-HA immunoprecipitates, myc-tagged LARG (myc-LARG) was detected. Conversely, in the myc-LARG immunoprecipitates, Unc5B-HA was detected. The interaction between these molecules in rat cortical neurons was also confirmed (Fig. 4 G).

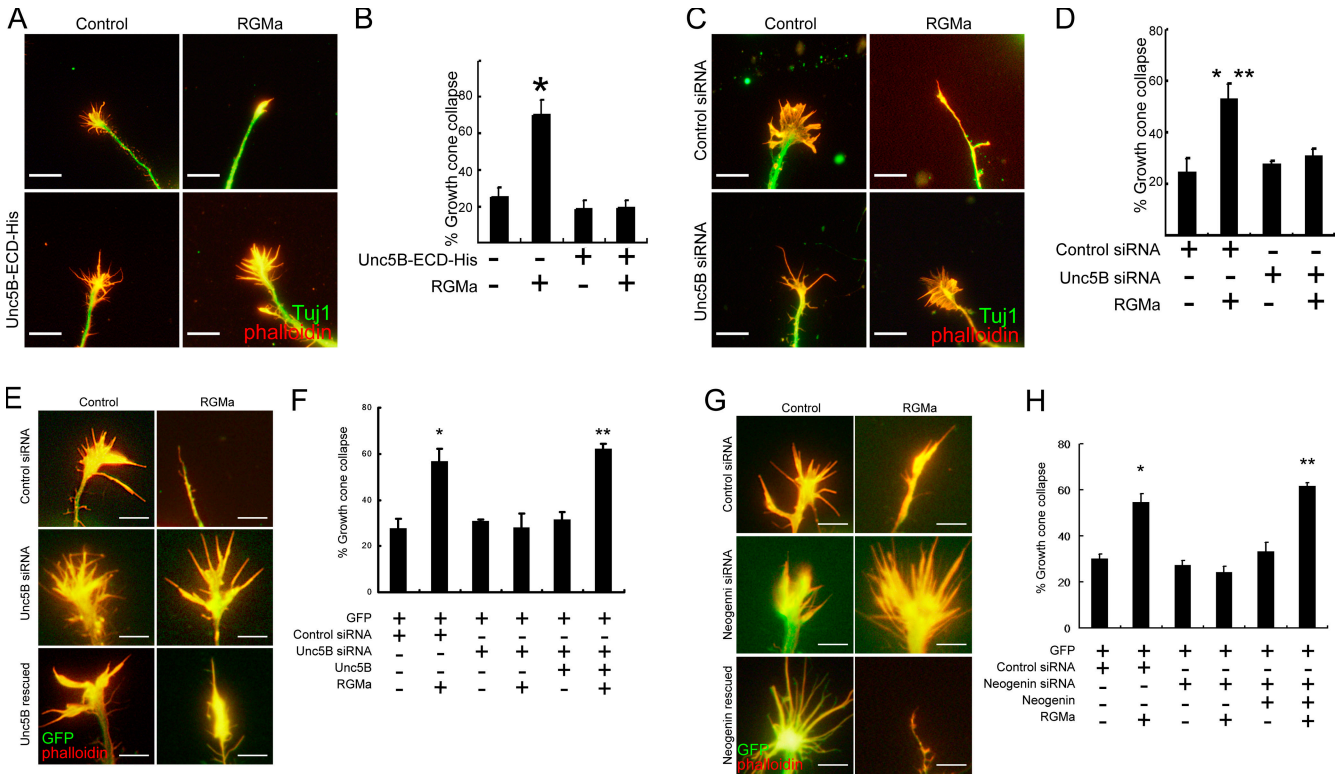

Figure 3. **Unc5B is required for growth cone collapse elicited by RGMa.** (A) Effects of Unc5B-ECD-His on RGMa-induced growth cone collapse. (B) The results from A were quantified from three independent experiments, and the percentage of collapsed growth cones is shown. *, $P < 0.01$ compared with Unc5B-ECD-His(−)/RGMa(−) or (+)/(+). (C) Effects of knockdown of Unc5B expression on RGMa-induced growth cone collapse in cortical neurons. (D) The results from C were quantified from three independent experiments, and the percentage of collapsed growth cones is shown. *, $P < 0.01$ compared with control siRNA(+)/Unc5 siRNA(−)/RGMa(−); **, $P < 0.05$ compared with (−)/(+)/(+). (E) Unc5B siRNA rescue experiment. Neurons were cotransfected with control siRNA + GFP construct, Unc5B siRNA + GFP construct, or Unc5B siRNA + Unc5B-HA + GFP constructs. (F) The results from E were quantified from three independent experiments, and the percentage of collapsed growth cones is shown. *, $P < 0.05$ compared with GFP(+)/control siRNA(+)/Unc5B siRNA(−)/Unc5B(−)/RGMa(−) or (+)/(−)/(+)/(−)/(+); **, $P < 0.01$ compared with (+)/(−)/(+)/(+)/(−). (G) Effects of knockdown of neogenin expression on growth cone collapse by RGMa in cortical neurons. (H) The results from G were quantified from three independent experiments, and the percentage of collapsed growth cones is shown. *, $P < 0.01$ compared with GFP(+)/control siRNA(+)/neogenin siRNA(−)/neogenin(−)/RGMa(−) or (+)/(−)/(+)/(−)/(+); **, $P < 0.01$ compared with (+)/(−)/(+)/(+)/(−). Error bars indicate SEM. Bars: (A and C) 10 µm; (E and G) 5 µm.

RGMa-dependent alteration of the interaction was not detected under the condition described in Fig. 4 G. This result is similar to those of previous studies in which the interaction of LARG with the IGF-1 receptor or with plexin-B1 was observed in the absence of a ligand, indicating that the interaction was constitutive (Taya et al., 2001; Aurandt et al., 2002; Driessens et al., 2002; Swiercz et al., 2002).

To characterize this interaction in detail, we sought to identify the domains in LARG that were required for the interaction. Previous studies show that LARG interacts with plexin-B1 or IGF-1 receptor via its PDZ domain (Taya et al., 2001; Hirotani et al., 2002; Swiercz et al., 2002). Therefore, we predicted that the LARG PDZ domain was important for the binding to Unc5B. IP was performed using lysates of 293T cells transfected with the mock construct, Unc5B-HA plus myc-LARG (full-length LARG), or Unc5B-HA plus myc-LARGΔPDZ (mutant LARG lacking the PDZ domain; Fig. 4 C). The full-length LARG precipitated Unc5B, whereas the deletion of the PDZ domain abolished the precipitation. We also demonstrated the specific interaction of Unc5B with the PDZ domain of LARG (myc–LARG PDZ) in transfected 293T cells (Fig. 4 D). These findings support our hypothesis that the PDZ domain of LARG binds to Unc5B. To identify the domains in Unc5B responsible for this interaction, we investigated the interaction of Unc5B with the PDZ domain of LARG in a GST pull-down assay using various deletion constructs of Unc5B ICD, as shown in Fig. 1 L and Fig. 4 E. Unc5B intracellular mutants containing the DD (Unc5B ICD-HA and Unc5B DD-HA) were found to specifically interact with GST–LARG PDZ. In contrast, the mutants lacking DD (Unc5B ZU5-HA and Unc5B ZU5/DB-HA) were not bound to GST–LARG PDZ, indicating that DD of Unc5B was required and sufficient for the interaction of Unc5B with LARG. Moreover, no association of neogenin-ICD with LARG PDZ was detected in the GST pull-down assay (Fig. 4 F). These results suggested the possibility that Unc5B acts as a signal transducer of RGMa by binding to LARG.

LARG is involved in RGMa-dependent RhoA activation

To evaluate the potential role of LARG in RGMa–neogenin–Unc5B-induced RhoA activation, we first used siRNA specific for LARG. Both neogenin–VSV-G– and Unc5B-HA–overexpressing 293T cells were cotransfected with control siRNA or LARG siRNA (Wang et al., 2004a,b). After 72 h, the cells were treated

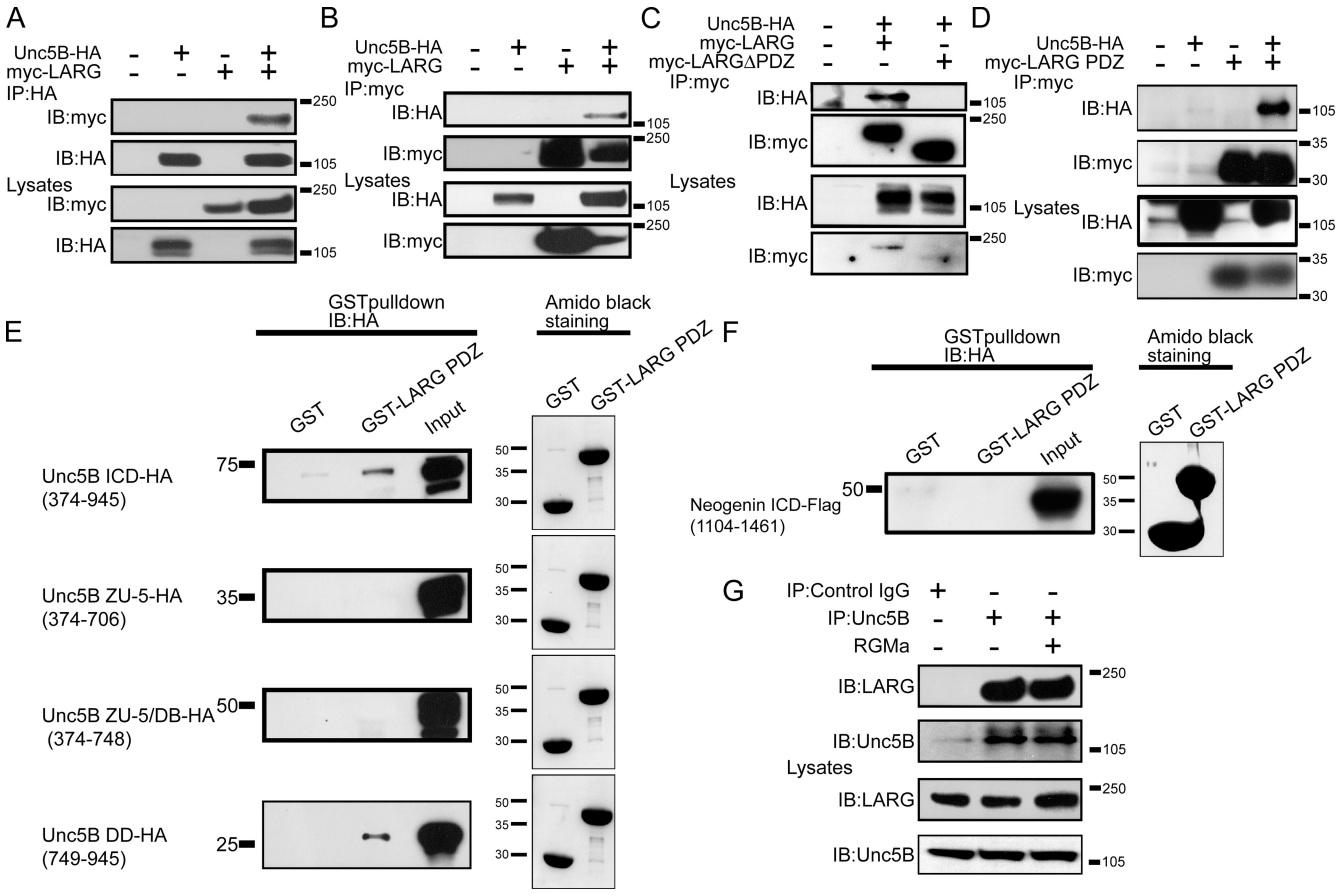

Figure 4. **Interaction of Unc5B with LARG.** (A and B) Co-IP of Unc5B with LARG in the transfected 293T cells. (C) Myc-LARGΔPDZ was not coimmunoprecipitated with Unc5B-HA in transfected 293T cells. The precipitated proteins with anti-myc antibody were immunoblotted with anti-HA or anti-myc antibody. (D) Co-IP of Unc5B-HA with myc–LARG PDZ in transfected 293T cells. (E and F) GST pull-down assay of GST–LARG PDZ with various deletion mutants of Unc5B ICD (E; Fig. 1 L) and with Flag-tagged neogenin-ICD (F; neogenin-ICD-Flag). An anti-HA or Flag antibody was used for the detection of proteins bound to the beads. (G) Co-IP of Unc5B with LARG in rat cortical neurons. Lysates were immunoprecipitated with anti-Unc5B antibody (IP:Unc5B) or control IgG (IP:Control IgG). IB, immunoblotting.

with 2 μg/ml RGMa or control medium for 15 min, and the RhoA activation assay was performed (Fig. 5 A). Significant RGMa-induced RhoA activation was detected in the control siRNA–transfected cells, whereas this activation was blocked by transfection with LARG siRNA (Fig. 5, A and B). Consistent with this finding, RGMa-induced RhoA activation was significantly abolished in LARG siRNA–transfected rat cortical neurons but not in those transfected with control siRNA (Fig. 5, E and F). To test the specificity of LARG siRNA, we performed rescue experiments in the knocked-down neurons. A total of 72 h after transfection with myc-LARG or the mock construct into LARG knocked-down neurons, cells were treated with 2 μg/ml RGMa or control medium for 15 min and subjected to the RhoA activation assay (Fig. 5, G and H). The overexpression of myc-LARG rescued RGMa-induced RhoA activation in LARG siRNA–transfected neurons, whereas the transfection of the mock construct did not, suggesting that the ability of knockdown of LARG to block RGMa-induced RhoA activation reflects loss of the targeted LARG and is not an off-target effect. These findings suggested that the presence of LARG was important for RGMa-dependent RhoA activation.

We next determined whether the recombinant PDZ domain of LARG (myc–LARG PDZ) blocked RGMa-induced RhoA activation presumably by inhibiting the association of LARG with Unc5B. To address this question, we cotransfected myc–LARG PDZ into neogenin–Unc5B-expressing 293T and COS-7 cells (Fig. 5 C). RhoA activation assays revealed that transfection with LARG PDZ inhibited RhoA activation by RGMa, indicating that LARG PDZ functions as the dominant-negative form of LARG (Fig. 5, C and D). Thus, these results support the notion that LARG regulates RGMa-dependent RhoA activation.

LARG mediates RGMa-induced growth cone collapse

We examined the role of LARG in RGMa-elicited growth cone collapse. To determine whether myc–LARG PDZ blocked the growth cone collapse induced by RGMa, we transfected cortical neurons with a vector encoding LARG PDZ. Cortical neurons were transfected with a GFP-encoding vector either alone or together with a myc–LARG PDZ–expressing plasmid. Furthermore, 48 h after the transfection, the growth cone collapse assay was performed. As shown in Fig. 6 (A and B), RGMa significantly increased the percentage of GFP-transfected cortical neurons showing growth cone collapse, and this increase was significantly reduced in the neurons cotransfected with GFP and

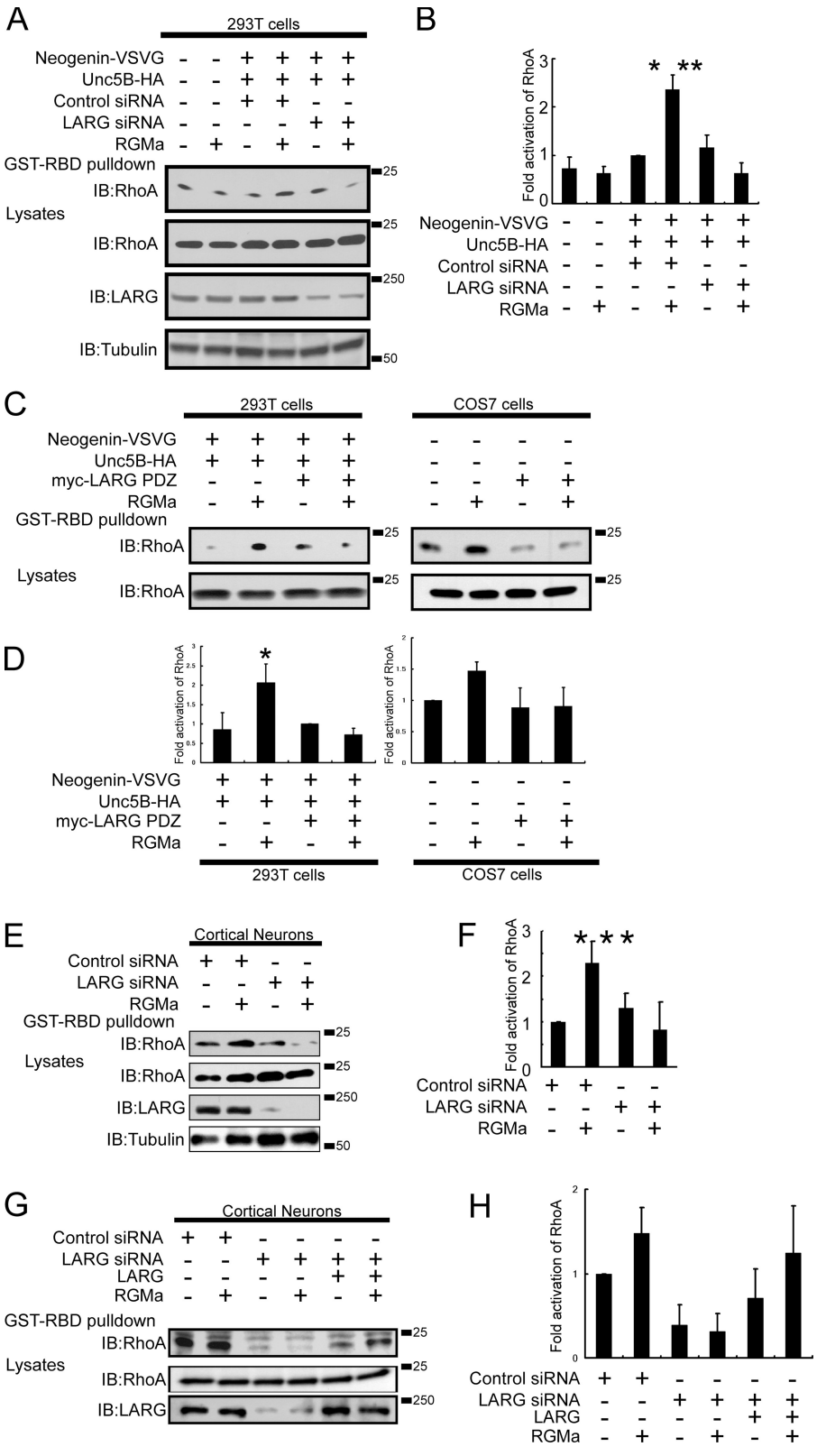

Figure 5. **Involvement of LARG in RhoA activation by RGMa.** (A) Effects of knockdown of endogenous LARG expression using siRNA on RhoA activation by RGMa in transfected 293T cells. (B) The quantification of the data shown in A from six independent experiments. *, $P < 0.01$ compared with neogenin–VSV-G(+)/Unc5B-HA(+)/control siRNA(+)/LARG siRNA(−)/RGMa(−); **, $P < 0.01$ compared with (+)/(+)/(−)/(+)/(+). (C) Effects of myc–LARG PDZ transfection on RhoA activation induced by RGMa in neogenin–Unc5B-expressing 293T cells (left) and COS-7 cells (right). (D) Quantification of the data shown in C from three independent experiments. *, $P < 0.05$ compared with neogenin–VSV-G(+)/Unc5B-HA(+)/myc–LARG PDZ(−)/RGMa(−) or (+)/(+)/(+)/(+). (E) The RhoA activation assay in cortical neurons knocked down for LARG by siRNA. Western blots of the lysates panel show the knockdown of LARG expression by LARG siRNA but not by control siRNA. (F) Quantification of the data shown in E from four independent experiments. *, $P < 0.05$ compared with control siRNA(+)/LARG siRNA(−)/RGMa(−); **, $P < 0.01$ compared with (−)/(+)/(+). (G) LARG siRNA rescue experiment. Neurons were cotransfected with control siRNA and mock construct, LARG siRNA and mock construct, or LARG siRNA and myc-LARG construct. Western blots of the lysates panel show that knockdown of LARG expression by LARG siRNA was rescued by transfection of a plasmid encoding myc-LARG but not by mock plasmid. (H) The quantification of the data shown in G from three independent experiments. IB, immunoblotting; RBD, GST-rhotekin-Rho–binding domain. Error bars indicate SEM.

myc–LARG PDZ. We further tested whether growth cone collapse was also blocked by LARG siRNA. Cortical neurons transfected with LARG siRNA or control siRNA were stimulated with 2 μg/ml RGMa or control medium and subjected to the growth cone collapse assay. As shown in Fig. 6 (C and D), LARG siRNA transfection specifically and significantly inhibited RGMa-mediated growth cone collapse. The specificity of LARG siRNA was confirmed in the rescue experiment by using GFP, myc-LARG, and mock constructs (Fig. 6, E and F). These findings indicated that LARG participated in RGMa-induced growth cone collapse.

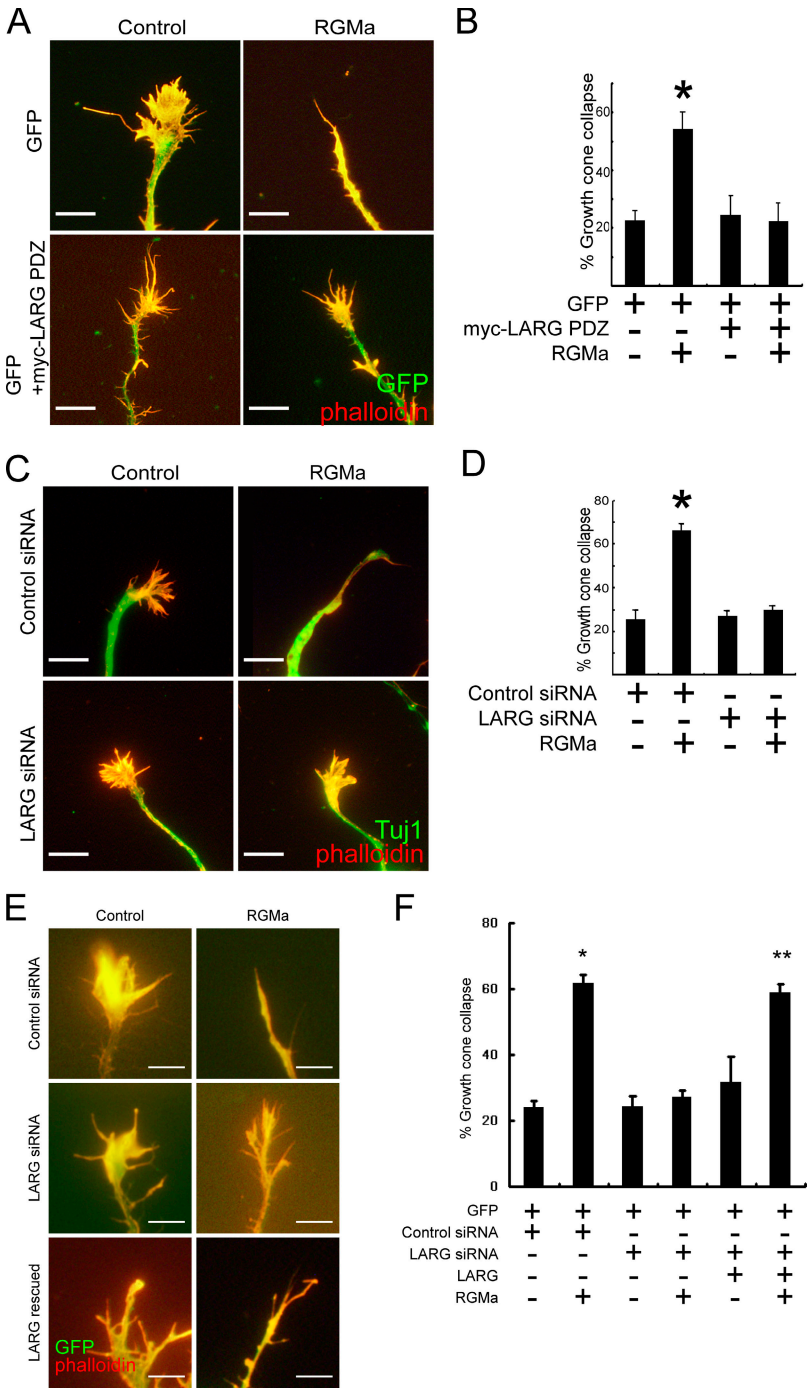

Figure 6. **Involvement of LARG in growth cone collapse by RGMa.** (A) Effects of myc–LARG PDZ on RGMa-induced growth cone collapse. (B) The results from A were quantified from three independent experiments, and the percentage of collapsed growth cones is shown. *, $P < 0.05$ compared with GFP(+)/myc–LARG PDZ (−)/RGMa(−) or (+)/(+)/(+). (C) The growth cone collapse assay in cortical neurons knocked down for LARG by siRNA. (D) The percentage of collapsed growth cones in three independent experiments. *, $P < 0.01$ compared with control siRNA(+)/LARG siRNA(−)/RGMa(−) or (−)/(+)/(+). (E) LARG siRNA rescue experiment. Neurons were cotransfected with control siRNA + GFP construct, LARG siRNA + GFP construct, or LARG siRNA + myc-LARG + GFP constructs. 72 h later, the growth cone collapse assay was performed. (F) The results from E were quantified from three independent experiments. *, $P < 0.01$ compared with GFP(+)/control siRNA(+)/LARG siRNA(−)/LARG(−)/RGMa(−) or (+)/(−)/(+)/(−)/(+); **, $P < 0.01$ compared with (+)/(−)/(+)/(+)/(−). Error bars indicate SEM. Bars: (A and C) 10 μm; (E) 5 μm.

FAK is involved in RGMa-dependent tyrosine phosphorylation of LARG and RhoA activation

Unc5B constitutively interacts with LARG via Unc5B DD and the LARG PDZ domain. Because the recombinant PDZ domain of LARG functions as a dominant-negative regulator of the RGMa signal, the association of Unc5B with LARG is considered to be necessary for RGMa-dependent RhoA activation. However, similar to previous studies (Taya et al., 2001; Aurandt et al., 2002; Driessens et al., 2002; Swiercz et al., 2002), the association of Unc5B with LARG was constitutive. Thus, the mechanism of RGMa-induced activation of RhoA by LARG cannot be explained by alteration of association of Unc5B with LARG in the ligand-dependent manner. We attempted to obtain more insight into the mechanism of LARG-mediated RhoA activation. FAK has been shown to interact with neogenin as well as DCC and mediate netrin-1–induced outgrowth of cortical axons (Li et al., 2004; Liu et al., 2004; Ren et al., 2004). Netrin-1 binding to DCC induces tyrosine phosphorylation of FAK. Activation of RhoA by LARG and PDZ-RhoGEF is enhanced when they are tyrosine phosphorylated by FAK (Chikumi et al., 2002a). Moreover, when the cells are treated with RGMa, FAK is dephosphorylated at Tyr-397 (our unpublished observations). These findings prompted

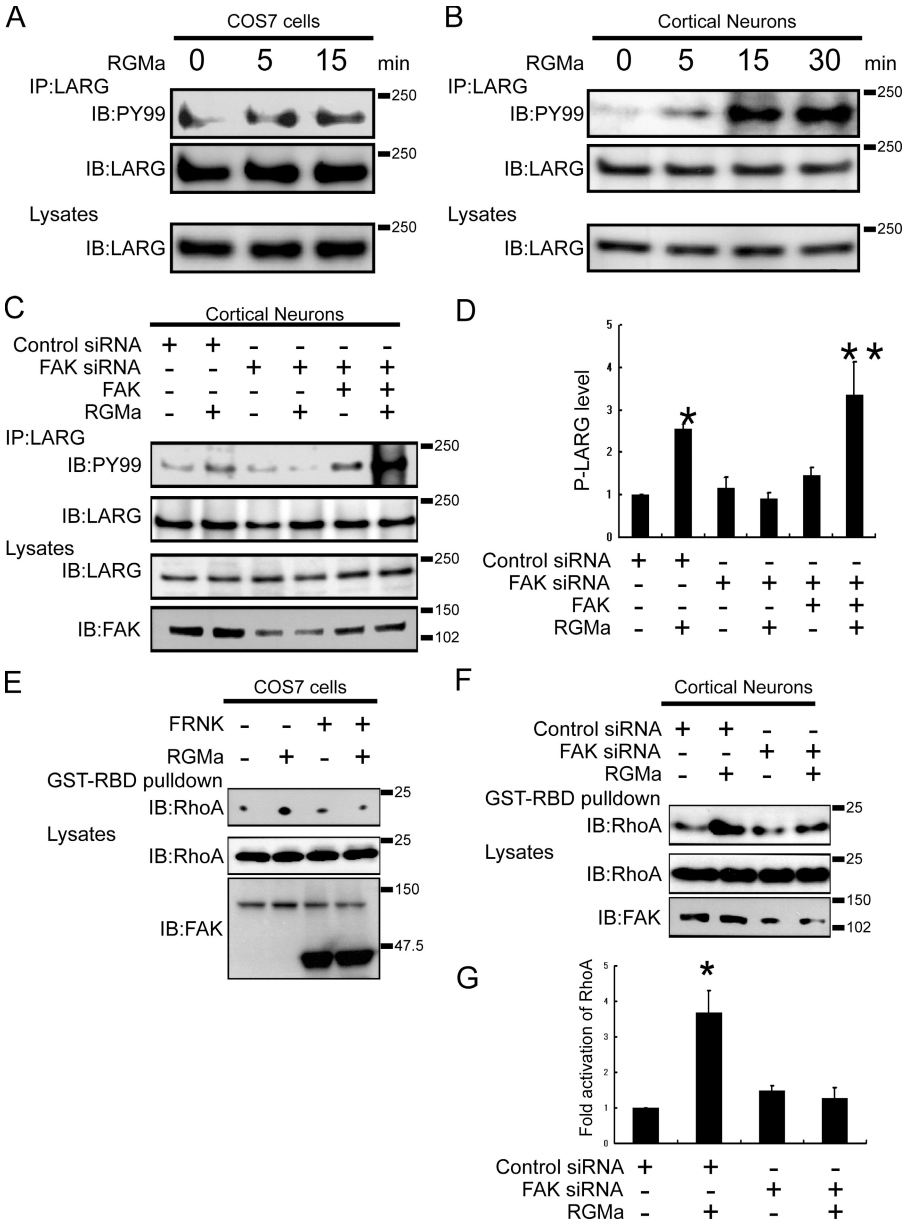

Figure 7. **FAK is involved in RGMa-induced tyrosine phosphorylation of LARG and RhoA activation.** (A and B) Increase in tyrosin phosphorylation of LARG after 2 µg/ml RGMa treatment in COS-7 cells (A) and cortical neurons (B). Lysates were immunoprecipitated with anti-LARG antibody and subjected to immunoblot analyses with antiphosphotyrosine antibody (IB: PY99) and anti-LARG antibody. (C) Effects of knockdown of FAK expression on tyrosin phosphorylation of LARG by RGMa in cortical neurons. Western blots of the lysates panel show that knockdown of FAK expression by FAK siRNA was rescued by transfection of a plasmid encoding HA-FAK. (D) The quantification of the data in C from three independent experiments (see Materials and methods). *, $P < 0.05$ compared with control siRNA(+)/FAK siRNA(−)/FAK(−)/RGMa(−) or (−)/(+)/(−)/(+); **, $P < 0.05$ compared with (−)/(+)/(+)/(−). (E) Effects of FRNK on RhoA activation induced by RGMa in COS-7 cells. COS-7 cells were mock transfected or transfected with myc-tagged FRNK. An anti-FAK immunoblot shows the expression of endogenous FAK and transfected myc-FRNK in total lysates. (F) Effects of knockdown of FAK expression on RhoA activation by RGMa in cortical neurons. (G) The quantification of the data shown in F from three independent experiments. *, $P < 0.01$ compared with control siRNA(+)/FAK siRNA(−)/RGMa(−) or (−)/(+)/(+). Error bars indicate SEM. IB, immunoblotting; P-LARG, phosphorylated LARG; RBD, GST-rhotekin-Rho–binding domain.

us to examine whether FAK modulated the function of LARG in the RGMa signaling pathway.

We first measured the tyrosine phosphorylation of LARG in cortical neurons and COS-7 cells. After stimulation with 2 µg/ml RGMa or control medium for 15 min, cells were lysed, subjected to IP with anti-LARG antibody, and further analyzed for the level of tyrosine-phosphorylated LARG by Western blotting with antiphosphotyrosine antibody (Fig. 7, A and B). We observed time-dependent induction of tyrosine phosphorylation of LARG after 2 µg/ml RGMa treatment in COS-7 cells and cortical neurons. To examine whether FAK mediates RGMa-induced tyrosine phosphorylation of LARG, we performed knockdown experiments for endogenous FAK by using siRNA in cortical neurons. The siRNA target sequence that has a strong knockdown effect on endogenous rat FAK expression has already been reported (Basson et al., 2006). A total of 72 h after transfection with FAK siRNA or control siRNA, neurons were treated with 2 µg/ml RGMa or control medium for 15 min, and the level of tyrosine-phosphorylated LARG was assessed. As shown in Fig. 7 (C and D), transfection with FAK siRNA and mock construct specifically and significantly inhibited RGMa-mediated tyrosine phosphorylation of LARG, whereas transfection with control siRNA and mock construct did not. The overexpression of HA-FAK in FAK siRNA–transfected neurons rescued RGMa-induced tyrosine phosphorylation of LARG, suggesting that the ability of knockdown of LARG to block RGMa-induced RhoA activation is not a result of an off-target effect of the siRNA. These results suggest that LARG is phosphorylated on tyrosine by FAK after stimulation with RGMa.

Finally, we examined the involvement of FAK in RGMa-induced RhoA activation. To disrupt endogenous FAK signaling, we used a truncated form of FAK termed FAK-related nonkinase (FRNK), which corresponds to the C-terminal domain

(aa 693–1,052) of FAK and functions as a dominant-negative form (Richardson and Parsons, 1996). As shown in Fig. 7 E, overexpression of FRNK resulted in the inhibition of RGMa-elicited RhoA activation in COS-7 cells. Furthermore, we observed that the RGMa-elicited RhoA activation in cortical neurons was inhibited by the transfection of FAK siRNA (Fig. 7, F and G). Thus, FAK participates in RGMa-induced RhoA activation.

Discussion

RGMa acts as a repulsive guidance cue for growing neurites and plays an important role in limiting CNS regeneration in vivo (Monnier et al., 2002; Brinks et al., 2004; Hata et al., 2006; Matsunaga et al., 2006; Wilson and Key, 2006; Tassew et al., 2008). It induces growth cone collapse or neurite growth inhibition in vitro (Monnier et al., 2002; Rajagopalan et al., 2004; Hata et al., 2006; Conrad et al., 2007; Kubo et al., 2008; Metzger et al., 2007). Neogenin was identified as the receptor for RGMa (Rajagopalan et al., 2004), and several intracellular signals, including RhoA/Rho kinase, PKC, and myosin IIA were found to be activated downstream of neogenin (Hata et al., 2006; Conrad et al., 2007; Kubo et al., 2008). However, the mechanism via which the binding of RGMa to neogenin activates the RhoA/Rho kinase pathway remained to be clarified. In this study, we showed that Unc5B interacted with neogenin and acted as a coreceptor for RGMa and associated with LARG to mediate RhoA activation and growth cone collapse. Furthermore, we revealed that FAK was involved in RGMa-induced tyrosine phosphorylation of LARG as well as RhoA activation.

Coreceptor system as the signal transducer of RGMa

Neogenin is a member of the DCC receptor family (Vielmetter et al., 1994; Keeling et al., 1997; Meyerhardt et al., 1997; Rajagopalan et al., 2004). Our finding that neogenin associates with Unc5 is similar to the well-established observation that DCC complexes with Unc5 to form a receptor complex for netrin-1 (Hong et al., 1999). In contrast to the observations that netrin-1 stimulation is required for this complex formation and that netrin-1 is a ligand of both receptors, the association of neogenin and Unc5B is ligand independent, and RGMa directly interacts with neogenin but not with Unc5B. Therefore, neogenin acts as a binding partner of its ligand, RGMa, whereas Unc5B may function as a signal-transducing element by binding with LARG. As the association of these receptors is constitutive, it remains to be elucidated how the signal transduction of RGMa is initiated.

The selective knockdown of Unc5B suppressed RGMa-dependent RhoA activation and growth cone collapse (Fig. 2, J–M; and Fig. 3, C–F). A cursory examination of this result seems to suggest that other Unc5 family members do not contribute to RGMa signal transduction. However, the ECD, intracellular DB domain, and intracellular DD of Unc5B, which are important for the binding to neogenin or LARG, are highly conserved in all the members of the Unc5 family (Unc5A–D/Unc5h1–4; Engelkamp, 2002). In fact, neogenin interacted with Unc5A and Unc5C in transfected 293T cells (Fig. 1, C–F). Moreover, our preliminary data suggest the possibility that Unc5A mediates RGMa-induced RhoA activation (unpublished data). These findings indicate that other Unc5 family members may also interact with neogenin or LARG and transduce the signal from RGMa to RhoA. The results shown in Fig. 2 (J–M) may indicate that the total expression level of Unc5 family members (i.e., Unc5A + Unc5B + Unc5C + Unc5D) is important for the signaling from RGMa to RhoA. Further studies are required for the evaluation of the role of other Unc5 family members in the RGMa signaling pathway.

Involvement of RhoGEFs in the signal transduction of RGMa

LARG contains the PDZ, RGS, Dbl homology, and pleckstrin homology domains and shows a high level of sequence homology to PDZ-RhoGEF. For example, the PDZ domains of PDZ-RhoGEF and LARG, which are regarded as the binding regions for interaction with Unc5, show 75% identity (Kourlas et al., 2000). They are also functionally similar. Both are involved in the signal transduction of trimeric G protein–coupled receptor (GPCR; Fukuhara et al., 1999, 2000; Booden et al., 2002; Chikumi et al., 2002b) and the regulation of RhoA and growth cone morphology induced by semaphorin 4D and plexin-B1 (Aurandt et al., 2002; Driessens et al., 2002; Swiercz et al., 2002). Although these results suggest that PDZ-RhoGEF is also involved in RGMa signaling, the interaction of PDZ-RhoGEF with Unc5B or neogenin was not detected. In addition, the specific inhibition of LARG was sufficient to attenuate the effects mediated by RGMa in the cortical neurons as well as in 293T and COS-7 cells. The participation of PDZ-RhoGEF in RGMa signaling should be addressed in the future.

Regulatory mechanism of FAK activity

We demonstrated that FAK mediated RGMa-induced tyrosine phosphorylation of LARG as well as RhoA activation. Because it has been reported that tyrosine phosphorylation of LARG by FAK results in the enhancement of RhoA activation (Chikumi et al., 2002a), the RhoGEF activity of LARG may be stimulated when LARG was tyrosine phosphorylated by FAK. However, it remains to be determined how RGMa binding to the receptor complex regulates the FAK activity.

An interesting hypothesis is the involvement of GPCRs in RGMa signaling. FAK was proposed to be activated by the heterotrimeric G protein α subunits $G\alpha_q$, $G\alpha_{12}$, and $G\alpha_{13}$, thereby enhancing the activation of Rho (Chikumi et al., 2002a). GPCRs may play a role in initiating RGMa signaling by activating FAK. In addition, FAK is dephosphorylated at Tyr-397 after cells are treated with RGMa (our unpublished observations). The tyrosine phosphatase responsible for FAK dephosphorylation, which is not yet identified, might regulate LARG phosphorylation by FAK as well as RhoA activation after the RGMa treatment. Elucidation of the regulatory mechanism of FAK in RGMa signaling is expected to provide a molecular basis for understanding the mechanism of neural wiring.

Materials and methods

Plasmid constructs

VSV-G–tagged human neogenin in pcDNA 3.1, the myc-tagged Unc5A in pSecTag B, HA-tagged rat Unc5B in pcDNA3.1, and myc-tagged Unc5C in pSecTag B were provided by E.R. Fearon (University of Michigan Medical School, Ann Arbor, Michigan), P. Mehlen (University of Lyon, Lyon, France), and L. Hinck (University of California, Santa Cruz, Santa Cruz, CA; Meyerhardt et al., 1997; Llambi et al., 2005; Bartoe et al., 2006). HA-FAK and myc-FRNK expression vectors were provided by M. Endo (Graduate School of Medicine, Kobe University, Kobe, Japan). By performing PCR on full-length constructs, we generated the following deletion mutants in mammalian expression vectors: neogenin-ICD-Flag in pSecTag2c/hygro (for the ICD of neogenin; aa 1,104–1,461; Invitrogen), GST-neogenin-ICD in pGEX-6P-3 (aa 1,127–1,461; GE Healthcare), HA-Unc5B-ECD in pcDNA 3.1(+) (for ECD of Unc5B; aa 1–396; Invitrogen), Unc5B-ECD-His in pSecTag2c/hygro (aa 1–373), Unc5B ICD-HA in pcDNA 3.1(+) (for ICD; aa 374–945), Unc5B-ZU5-HA in pSecTag2c/hygro (for the ZU5 domain; aa 374–706), Unc5B-ZU5/DB-HA in pSecTag2c/hygro (for the ZU5 and DB domains; aa 374–748), and Unc5B-DD-HA in pcDNA 3.1(+) (for DD; aa 749–945). The methods of constructing the plasmids pCMV-myc-LARG, pCMV-myc–LARG ΔPDZ, and pGEX5X-GST–LARG PDZ have been previously described (Hirotani et al., 2002). Myc–LARG PDZ in pcDNA3.1(+) (PDZ domain of LARG; aa 32–295) were generated using PCR with full-length LARG as the template. All PCR products were verified by sequencing.

Cell culture

HEK 293T or COS-7 cells were maintained and cultured in DME (Invitrogen) supplemented with 10% FBS. Cortical neurons obtained from rat pups on E19–20 were dissociated by trypsinization (treatment with 0.25% trypsin in PBS for 15 min at 37°C) followed by resuspension in DME/F12 (Invitrogen) containing 10% FBS and trituration. Subsequently, the neurons were washed three times. The cells were suspended in a serum-free DME/F12 medium supplemented with B27 (Invitrogen), plated on poly-L-lysine–coated dishes, and maintained at 37°C in 5% CO_2.

Lipofection with plasmids and/or siRNA

Transient transfection experiments with plasmids for HEK 293T and COS-7 cells were performed using Lipofectamine 2000 (Invitrogen) according to the manufacturer's recommendations. The cells were lysed 48 h after the transfection and used for IP, Rho activation assay, GST pull-down assay, or Western blotting.

The target sequence of the siRNA for human LARG and the methods of transfecting 293T cells have been previously described (Wang et al., 2004b). The duplex siRNA was synthesized by Greiner Bio-One.

ELISA

2 µg/ml human Unc5B-ECD-Fc (1006-UN; R&D Systems), 2 µg/ml RGMa (R&D Systems), or 2 µg/ml BSA diluted in 1% BSA/PBS was added to ELISA 96-well microplates (Thermo Fisher Scientific) coated with 0.5 µg/ml BSA, 0.5 µg/ml neogenin-ECD (Mitsubishi Tanabe Pharma Corp.), or 0.5 µg/ml Unc5B-ECD-Fc. Furthermore, 2 h after the incubation, the plates were washed, diluted, and anti-Unc5B (R&D Systems) or anti-RGMa (Hata et al., 2006) antibody was added. HRP-conjugated secondary antibody and substrate reagent pack and stop solutions (R&D Systems) were used for detection. The absorbancy at 450 nm was measured. As shown in Fig. 1 G, statistical analysis of the values was performed using one-way analysis of variance (ANOVA) followed by Scheffe's multiple comparison test.

Nucleofection of rat cortical neurons

To knock down the expression of Unc5B or LARG in rat cortical neurons, the following siRNA were used: rat Unc5B (SMARTpool or ON-TARGET plus SMARTpool; Thermo Fisher Scientific), rat LARG (ON-TARGET plus SMARTpool), rat neogenin (ON-TARGET plus SMARTpool), and rat FAK (Basson et al., 2006). The ON-TARGET plus SMARTpool siRNA is a mixture of four individual siRNA duplexes. Freshly isolated rat cortical neurons were suspended in 100 µl transfection solution (Amaxa Biosystems) containing 500 pmol of the various siRNA duplexes or control nontargeting siRNA. The cell suspension was nucleofected using program O-03 (Amaxa Biosystems) according to the manufacturer's protocol. After the addition of 1 ml DME/F12 supplemented with 10% FBS, neurons were plated on poly-L-lysine–coated dishes. The culture medium was replaced with serum-free DME/F12 supplemented with B27 3 h after plating. For the siRNA rescue experiments in biochemical assays, neurons were cotransfected with 250 pmol siRNA oligonucleotides and 2.5 µg of appropriate plasmid constructs. For the siRNA rescue experiments in the growth cone collapse assay, the ratio of the number of GFP/plasmid (Amaxa Biosystems) and each plasmid construct was 1:10. For the transfection of GFP and/or myc–LARG PDZ into cortical neurons, 0.4 µg of a vector encoding GFP and/or 4.4 µg of a myc–LARG PDZ vector was electroporated. Furthermore, 48 (the transfection of GFP and/or myc–LARG PDZ) or 72 h (the transfection of siRNA) after the transfection, the cells were subjected to IP, Rho activation assay, Western blotting, or growth cone collapse assay.

Co-IP assay

The transfected 293T cells or rat cortical neurons were lysed in 50 mM Tris-HCl, pH 7.5, 150 mM NaCl, 10% glycerol, and 1% NP-40 supplemented with protease inhibitor cocktail tablets (Roche). The lysates were incubated on a rocking platform at 4°C for 20 min and clarified by centrifugation at 13,000 *g* at 4°C for 10 min. The supernatants collected were precleared for 30 min by incubating with 60 µl protein A/G–Sepharose beads (GE Healthcare). After a brief centrifugation to remove the precleared beads, the cell lysates were incubated for 2 h (for co-IP with transfected 293T cell extracts) or overnight (for co-IP with rat cortical neuron extracts) at 4°C with anti–VSV-G antibody (Sigma-Aldrich), anti-HA antibody (Sigma-Aldrich), anti–c-myc antibody (Santa Cruz Biotechnology, Inc.), antineogenin (Santa Cruz Biotechnology, Inc.), anti-Unc5B (R&D Systems), or anti-LARG antibody (Santa Cruz Biotechnology, Inc.). The immunocomplexes were collected for 1 h at 4°C by using the protein A/G–Sepharose beads, which had been coated with 0.1% BSA in PBS. The beads were washed four times with the lysis buffer. The bound proteins were solubilized with 2× sample buffer and subjected to SDS-PAGE followed by immunoblotting.

GST pull-down assay

GST pull-down assay was performed as described previously (Zhu et al., 2007). The 293T cells transfected with plasmids encoding neogenin-ICD-Flag or various fragments of the HA-tagged Unc5B ICD (Fig. 1 L) were lysed in 50 mM Tris, pH 7.5, 150 mM NaCl, and 0.2% NP-40 in the presence of protease inhibitors, subjected to sonication, and centrifuged at 13,000 *g* for 10 min. The supernatant was precleared for 1 h at 4°C with glutathione–Sepharose 4B beads (GE Healthcare). After centrifugation, the supernatant was incubated for 2 h at 4°C with the various GST-fused proteins that were immobilized on glutathione–Sepharose 4B beads. The resultant beads were washed four times, eluted in 2× sample buffer, and subjected to SDS-PAGE and immunoblotting with anti-Flag or anti-HA antibody.

Production of recombinant Unc5B-ECD-His

To generate soluble His-tagged Unc5B-ECD–expressing CHO cells (Unc5B-ECD-His–CHO cells), the Flp-In system (Invitrogen) was used according to the manufacturer's recommendations. To collect secreted Unc5B-ECD-His, the conditioned medium of Unc5B-ECD-His–CHO cells was incubated for 1 h at 4°C with nickel nitrilotriacetic acid agarose beads (Invitrogen). After washing the beads with a buffer containing 10 mM imidazole, His-tagged proteins were eluted with 300 mM imidazole, concentrated in Amicon Ultra concentrators (10K; Millipore) as instructed by the manufacturers, and diluted in PBS. Recombinant soluble His-tagged TrkB ECD (R&D Systems) was used as a negative control in the rhotekin pull-down assay.

Treatment of cells with recombinant Unc5B-ECD-His or TrkB-His

COS-7 cells or neurons were cultured for 48 h in the presence of 2 µg/ml Unc5B-ECD-His, 2 µg/ml TrkB-His (1494-TB; R&D Systems), or control solution, treated with 2 µg/ml RGMa or control medium for 15 or 30 min, and subjected to IP, Rho activation assay, Western blotting, or growth cone collapse assay.

Affinity precipitation of GTP-RhoA

After stimulation with 2 µg/ml recombinant RGMa (R&D Systems) or control medium for 15 min, cells were lysed in a solution containing 50 mM Tris, pH 7.5, 1% NP-40, 5% glycerol, 1 mM Na_3VO_4, 1 mM NaF, 150 mM NaCl, 30 mM $MgCl_2$, 1 mM DTT, and 10 µg/ml each of leupeptin and aprotinin. The cell lysates were clarified by centrifugation at 13,000 *g* at 4°C for 10 min, and the supernatants were incubated with 20 µg GST-rhotekin-Rho–binding domain beads (Ren and Schwartz, 2000) at 4°C for 45 min. The beads were washed four times with the lysis buffer and subjected to SDS-PAGE followed by immunoblotting with anti-RhoA antibody (Santa Cruz Biotechnology, Inc.). The cell lysates were also immunoblotted for total RhoA. The levels of RhoA activation were calculated by comparing the band intensities of active RhoA bands with those of total RhoA in each

lane using Scion Image software (Scion Corporation). The values obtained were then divided by those of control, and the results were expressed in terms of fold increases. The quantitative data are expressed as the means of at least three independent experiments ± SEM. Statistical analysis of the values was performed using one-way ANOVA followed by Scheffe's (Fig. 5 B), Tukey's (Fig. 2, B and I; and Fig. 7 G), or Holm's (Fig. 2, G, K, and M; and Fig. 5, D and F) multiple comparison test.

Western blot analysis

The protein samples were boiled in sample buffer for 5 min, run on SDS-PAGE, and transblotted to PVDF membranes. The membranes were blocked for 1 h at room temperature with 0.5% skim milk, incubated for 1 h at room temperature with anti–VSV-G (1:1,000 dilution; Sigma-Aldrich), monoclonal anti-HA (1:20,000 dilution; Sigma-Aldrich), polyclonal anti-HA (1:20,000 dilution; Abcam), anti–c-myc (1:1,000 dilution; Santa Cruz Biotechnology, Inc.), antineogenin (1:1,000 dilution; Santa Cruz Biotechnology, Inc.), anti-Unc5A (1:1,000 dilution; Millipore), anti-Unc5B (1:1,000 dilution; R&D Systems), anti-Unc5C (1:1,000 dilution; R&D Systems), anti-LARG (1:1,000 dilution; Santa Cruz Biotechnology, Inc.), anti-RhoA (1:1,000 dilution; Santa Cruz Biotechnology, Inc.), anti–glyceraldehyde 3-phosphate dehydrogenase (1:1,000 dilution; Santa Cruz Biotechnology, Inc.), antitubulin (1:1,000 dilution; Santa Cruz Biotechnology, Inc.), antiphosphotyrosine (PY99; 1:1,000 dilution; Santa Cruz Biotechnology, Inc.), or 10 µg/ml anti-Flag (Sigma-Aldrich) antibody. HRP-conjugated secondary antibodies and ECL plus reagents (GE Healthcare) were used for detection. Membrane was exposed to x-ray film or an image system (LAS-3000; Fujifilm) according to the manufacturer's specifications.

The detection of the level of tyrosine-phosphorylated LARG

After treatment with 2 µg/ml RGMa or control medium for 15 min, cells were lysed in 50 mM Tris-HCl, pH 7.5, 150 mM NaCl, 10% glycerol, and 1% NP-40 supplemented with protease inhibitor cocktail tablets (Roche). The lysates were incubated on a rocking platform at 4°C for 10 min and clarified by centrifugation at 13,000 *g* at 4°C for 10 min. The supernatants collected were incubated for 2 h at 4°C with anti-LARG (Santa Cruz Biotechnology, Inc.) antibody. The immunocomplexes were collected for 1 h at 4°C by using the protein G–Sepharose beads. The beads were washed four times with the lysis buffer. The bound proteins were solubilized with 2× sample buffer and subjected to SDS-PAGE followed by immunoblotting with antiphosphotyrosine (PY99) antibody (1:1,000 dilution; Santa Cruz Biotechnology, Inc.). As shown in Fig. 7 D, the relative levels of tyrosine phosphorylation of LARG are indicated by the amount of tyrosin-phosphorylated LARG normalized to the amount of immunoprecipitated LARG protein. The quantitative data are expressed as the means of three independent experiments ± SEM. Statistical analysis of the values was performed using one-way ANOVA followed by Holm's multiple comparison test.

Collapse assay

After treatment with 2 µg/ml RGMa or control medium for 30 min, cortical neurons were fixed for 30 min at room temperature with 0.5% glutaraldehyde (TAAB Laboratories). To visualize growth cones, neurons were stained with rhodamine-conjugated phalloidin (1:1,000 dilution; Invitrogen). In the assay with Unc5B-ECD-His–treated or Unc5B/LARG siRNA–transfected neurons, the neurons were also counterstained with anti-TuJ1 (1:5,000 dilution; Covance). Images were acquired on a microscope (BX51; Olympus) equipped with a camera (DP71; Olympus) using controller software (version 3.1.1.267; DP; Olympus). The UPlanSApo 40×/0.90 and UPlanSApo 100×/1.40 oil immersion objectives (Olympus) were used. The criterion for the collapsed growth cones was the loss of lamellipodia and two or fewer filopodia. In each experiment, 50 neurons were counted per group. To calculate the percentage of collapse, the number of collapsed growth cones was divided by the number of total growth cones. Data were collected from at least three independent experiments and expressed as means ± SEM. Statistical analysis was performed using one-way ANOVA followed by Scheffe's (Fig. 3, B and D; and Fig. 6 D), Tukey's (Fig. 3, F and H; and Fig. 6 F), or Holm's (Fig. 6 B) multiple comparison test.

We are very grateful to Dr. Patrick Mehlen, Dr. Lindsay Hinck, and Dr. Eric R. Fearon for providing the vectors encoding VSV-G–tagged human neogenin, myc-tagged Unc5A, HA-tagged rat Unc5B, and myc-tagged Unc5C, to Mitsubishi Tanabe Pharma Co. for providing neogenin-ECD, and to Dr. M. Endo for providing HA-FAK and myc-FRNK expression vectors. We also thank Hiroe Sakai for critical reading of the manuscript and valuable comments.

This work was supported by a research grant from the National Institute of Biomedical Innovation (05-12) and Grant-in-Aid for Young Scientists (S) from the Japan Society for the Promotion of Science.

Submitted: 7 July 2008
Accepted: 6 February 2009

References

Aurandt, J., H.G. Vikis, J.S. Gutkind, N. Ahn, and K.L. Guan. 2002. The semaphorin receptor plexin-B1 signals through a direct interaction with the Rho-specific nucleotide exchange factor, LARG. *Proc. Natl. Acad. Sci. USA.* 99:12085–12090.

Barallobre, M.J., M. Pascual, J.A. Del Rio, and E. Soriano. 2005. The Netrin family of guidance factors: emphasis on Netrin-1 signalling. *Brain Res. Brain Res. Rev.* 49:22–47.

Bartoe, J.L., W.L. McKenna, T.K. Quan, B.K. Stafford, J.A. Moore, J. Xia, K. Takamiya, R.L. Huganir, and L. Hinck. 2006. Protein interacting with C-kinase 1/protein kinase Calpha-mediated endocytosis converts netrin-1-mediated repulsion to attraction. *J. Neurosci.* 26:3192–3205.

Basson, M.D., M.A. Sanders, R. Gomez, J. Hatfield, R. Vanderheide, V. Thamilselvan, J. Zhang, and M.F. Walsh. 2006. Focal adhesion kinase protein levels in gut epithelial motility. *Am. J. Physiol. Gastrointest. Liver Physiol.* 291:G491–G499.

Booden, M.A., D.P. Siderovski, and C.J. Der. 2002. Leukemia-associated Rho guanine nucleotide exchange factor promotes G alpha q-coupled activation of RhoA. *Mol. Cell. Biol.* 22:4053–4061.

Brinks, H., S. Conrad, J. Vogt, J. Oldekamp, A. Sierra, L. Deitinghoff, I. Bechmann, G. Alvarez-Bolado, B. Heimrich, P.P. Monnier, et al. 2004. The repulsive guidance molecule RGMa is involved in the formation of afferent connections in the dentate gyrus. *J. Neurosci.* 24:3862–3869.

Chikumi, H., S. Fukuhara, and J.S. Gutkind. 2002a. Regulation of G protein-linked guanine nucleotide exchange factors for Rho, PDZ-RhoGEF, and LARG by tyrosine phosphorylation: evidence of a role for focal adhesion kinase. *J. Biol. Chem.* 277:12463–12473.

Chikumi, H., J. Vazquez-Prado, J.M. Servitja, H. Miyazaki, and J.S. Gutkind. 2002b. Potent activation of RhoA by Galpha q and Gq-coupled receptors. *J. Biol. Chem.* 277:27130–27134.

Conrad, S., H. Genth, F. Hofmann, I. Just, and T. Skutella. 2007. Neogenin-RGMa signaling at the growth cone is bone morphogenetic protein-independent and involves RhoA, ROCK, and PKC. *J. Biol. Chem.* 282:16423–16433.

Driessens, M.H., C. Olivo, K. Nagata, M. Inagaki, and J.G. Collard. 2002. B plexins activate Rho through PDZ-RhoGEF. *FEBS Lett.* 529:168–172.

Engelkamp, D. 2002. Cloning of three mouse Unc5 genes and their expression patterns at mid-gestation. *Mech. Dev.* 118:191–197.

Fukuhara, S., H. Chikumi, and J.S. Gutkind. 2000. Leukemia-associated Rho guanine nucleotide exchange factor (LARG) links heterotrimeric G proteins of the G(12) family to Rho. *FEBS Lett.* 485:183–188.

Fukuhara, S., C. Murga, M. Zohar, T. Igishi, and J.S. Gutkind. 1999. A novel PDZ domain containing guanine nucleotide exchange factor links heterotrimeric G proteins to Rho. *J. Biol. Chem.* 274:5868–5879.

Fukuhara, S., H. Chikumi, and J.S. Gutkind. 2001. RGS-containing RhoGEFs: the missing link between transforming G proteins and Rho? *Oncogene.* 20:1661–1668.

Gad, J.M., S.L. Keeling, A.F. Wilks, S.S. Tan, and H.M. Cooper. 1997. The expression patterns of guidance receptors, DCC and Neogenin, are spatially and temporally distinct throughout mouse embryogenesis. *Dev. Biol.* 192:258–273.

Hata, K., M. Fujitani, Y. Yasuda, H. Doya, T. Saito, S. Yamagishi, B.K. Mueller, and T. Yamashita. 2006. RGMa inhibition promotes axonal growth and recovery after spinal cord injury. *J. Cell Biol.* 173:47–58.

Hirotani, M., Y. Ohoka, T. Yamamoto, H. Nirasawa, T. Furuyama, M. Kogo, T. Matsuya, and S. Inagaki. 2002. Interaction of plexin-B1 with PDZ domain-containing Rho guanine nucleotide exchange factors. *Biochem. Biophys. Res. Commun.* 297:32–37.

Hong, K., L. Hinck, M. Nishiyama, M.M. Poo, M. Tessier-Lavigne, and E. Stein. 1999. A ligand-gated association between cytoplasmic domains of UNC5 and DCC family receptors converts netrin-induced growth cone attraction to repulsion. *Cell.* 97:927–941.

Keeling, S.L., J.M. Gad, and H.M. Cooper. 1997. Mouse Neogenin, a DCC-like molecule, has four splice variants and is expressed widely in the adult mouse and during embryogenesis. *Oncogene.* 15:691–700.

Kourlas, P.J., M.P. Strout, B. Becknell, M.L. Veronese, C.M. Croce, K.S. Theil, R. Krahe, T. Ruutu, S. Knuutila, C.D. Bloomfield, and M.A. Caligiuri. 2000. Identification of a gene at 11q23 encoding a guanine nucleotide exchange factor: evidence for its fusion with MLL in acute myeloid leukemia. *Proc. Natl. Acad. Sci. USA.* 97:2145–2150.

Kubo, T., M. Endo, K. Hata, J. Taniguchi, K. Kitajo, S. Tomura, A. Yamaguchi, B.K. Mueller, and T. Yamashita. 2008. Myosin IIA is required for neurite outgrowth inhibition produced by repulsive guidance molecule. *J. Neurochem.* 105:113–126.

Kuns-Hashimoto, R., D. Kuninger, M. Nili, and P. Rotwein. 2008. Selective binding of RGMc/hemojuvelin, a key protein in systemic iron metabolism, to BMP-2 and neogenin. *Am. J. Physiol. Cell Physiol.* 294:C994–C1003.

Lee, H.K., I.A. Seo, E. Seo, S.Y. Seo, H.J. Lee, and H.T. Park. 2007. Netrin-1 induces proliferation of Schwann cells through Unc5b receptor. *Biochem. Biophys. Res. Commun.* 362:1057–1062.

Li, W., J. Lee, H.G. Vikis, S.H. Lee, G. Liu, J. Aurandt, T.L. Shen, E.R. Fearon, J.L. Guan, M. Han, et al. 2004. Activation of FAK and Src are receptor-proximal events required for netrin signaling. *Nat. Neurosci.* 7:1213–1221.

Liu, G., H. Beggs, C. Jurgensen, H.T. Park, H. Tang, J. Gorski, K.R. Jones, L.F. Reichardt, J. Wu, and Y. Rao. 2004. Netrin requires focal adhesion kinase and Src family kinases for axon outgrowth and attraction. *Nat. Neurosci.* 7:1222–1232.

Llambi, F., F.C. Lourenco, D. Gozuacik, C. Guix, L. Pays, G. Del Rio, A. Kimchi, and P. Mehlen. 2005. The dependence receptor UNC5H2 mediates apoptosis through DAP-kinase. *EMBO J.* 24:1192–1201.

Manitt, C., K.M. Thompson, and T.E. Kennedy. 2004. Developmental shift in expression of netrin receptors in the rat spinal cord: predominance of UNC-5 homologues in adulthood. *J. Neurosci. Res.* 77:690–700.

Matsunaga, E., S. Tauszig-Delamasure, P.P. Monnier, B.K. Mueller, S.M. Strittmatter, P. Mehlen, and A. Chedotal. 2004. RGM and its receptor neogenin regulate neuronal survival. *Nat. Cell Biol.* 6:749–755.

Matsunaga, E., H. Nakamura, and A. Chedotal. 2006. Repulsive guidance molecule plays multiple roles in neuronal differentiation and axon guidance. *J. Neurosci.* 26:6082–6088.

Menard, C., P. Hein, A. Paquin, A. Savelson, X.M. Yang, D. Lederfein, F. Barnabe-Heider, A.A. Mir, E. Sterneck, A.C. Peterson, et al. 2002. An essential role for a MEK-C/EBP pathway during growth factor-regulated cortical neurogenesis. *Neuron.* 36:597–610.

Metzger, M., S. Conrad, T. Skutella, and L. Just. 2007. RGMa inhibits neurite outgrowth of neuronal progenitors from murine enteric nervous system via the neogenin receptor in vitro. *J. Neurochem.* 103:2665–2678.

Meyerhardt, J.A., A.T. Look, S.H. Bigner, and E.R. Fearon. 1997. Identification and characterization of neogenin, a DCC-related gene. *Oncogene.* 14:1129–1136.

Monnier, P.P., A. Sierra, P. Macchi, L. Deitinghoff, J.S. Andersen, M. Mann, M. Flad, M.R. Hornberger, B. Stahl, F. Bonhoeffer, and B.K. Mueller. 2002. RGM is a repulsive guidance molecule for retinal axons. *Nature.* 419:392–395.

Niederkofler, V., R. Salie, M. Sigrist, and S. Arber. 2004. Repulsive guidance molecule (RGM) gene function is required for neural tube closure but not retinal topography in the mouse visual system. *J. Neurosci.* 24:808–818.

Rajagopalan, S., L. Deitinghoff, D. Davis, S. Conrad, T. Skutella, A. Chedotal, B.K. Mueller, and S.M. Strittmatter. 2004. Neogenin mediates the action of repulsive guidance molecule. *Nat. Cell Biol.* 6:756–762.

Ren, X.D., and M.A. Schwartz. 2000. Determination of GTP loading on Rho. *Methods Enzymol.* 325:264–272.

Ren, X.R., G.L. Ming, Y. Xie, Y. Hong, D.M. Sun, Z.Q. Zhao, Z. Feng, Q. Wang, S. Shim, Z.F. Chen, et al. 2004. Focal adhesion kinase in netrin-1 signaling. *Nat. Neurosci.* 7:1204–1212.

Richardson, A., and T. Parsons. 1996. A mechanism for regulation of the adhesion-associated proteintyrosine kinase pp125FAK. *Nature.* 380:538–540.

Schmidtmer, J., and D. Engelkamp. 2004. Isolation and expression pattern of three mouse homologues of chick Rgm. *Gene Expr. Patterns.* 4:105–110.

Swiercz, J.M., R. Kuner, J. Behrens, and S. Offermanns. 2002. Plexin-B1 directly interacts with PDZ-RhoGEF/LARG to regulate RhoA and growth cone morphology. *Neuron.* 35:51–63.

Tassew, N.G., L. Chestopolava, R. Beecroft, E. Matsunaga, H. Teng, A. Chedotal, and P.P. Monnier. 2008. Intraretinal RGMa is involved in retino-tectal mapping. *Mol. Cell. Neurosci.* 37:761–769.

Taya, S., N. Inagaki, H. Sengiku, H. Makino, A. Iwamatsu, I. Urakawa, K. Nagao, S. Kataoka, and K. Kaibuchi. 2001. Direct interaction of insulin-like growth factor-1 receptor with leukemia-associated RhoGEF. *J. Cell Biol.* 155:809–820.

Vielmetter, J., J.F. Kayyem, J.M. Roman, and W.J. Dreyer. 1994. Neogenin, an avian cell surface protein expressed during terminal neuronal differentiation, is closely related to the human tumor suppressor molecule deleted in colorectal cancer. *J. Cell Biol.* 127:2009–2020.

Wang, Q., M. Liu, T. Kozasa, J.D. Rothestein, P.C. Sternweis, and R.R. Neubig. 2004a. Ribozyme- and siRNA-mediated suppression of RGS-containing RhoGEF proteins. *Methods Enzymol.* 389:244–265.

Wang, Q., M. Liu, T. Kozasa, J.D. Rothstein, P.C. Sternweis, and R.R. Neubig. 2004b. Thrombin and lysophosphatidic acid receptors utilize distinct rhoGEFs in prostate cancer cells. *J. Biol. Chem.* 279:28831–28834.

Williams, M.E., S.C. Wu, W.L. McKenna, and L. Hinck. 2003. Surface expression of the netrin receptor UNC5H1 is regulated through a protein kinase C-interacting protein/protein kinase-dependent mechanism. *J. Neurosci.* 23:11279–11288.

Wilson, N.H., and B. Key. 2006. Neogenin interacts with RGMa and netrin-1 to guide axons within the embryonic vertebrate forebrain. *Dev. Biol.* 296:485–498.

Zhu, X.J., C.Z. Wang, P.G. Dai, Y. Xie, N.N. Song, Y. Liu, Q.S. Du, L. Mei, Y.Q. Ding, and W.C. Xiong. 2007. Myosin X regulates netrin receptors and functions in axonal path-finding. *Nat. Cell Biol.* 9:184–192.